TITLE PAGE

KDM6B Regulates Prostate Cancer Cell Proliferation by Controlling c-MYC Expression

Gökçe Yıldırım-Buharalıoğlu[1]

[1]Faculty of Pharmacy, Department of Pharmacology, Ege University, Izmir,Turkey (GYB)

RUNNING TITLE PAGE

Corresponding author: Gökçe Yıldırım-Buharalıoğlu

Faculty of Pharmacy, Department of Pharmacology, Ege University, Erzene Mahallesi Ankara

Caddesi No:172/98, Bornova, Izmir, TURKEY, Post code: 35040, Tel: (+90)232 3114072,

E-mail: yildirim5559@hotmail.com

The number of text pages: 35

The number of tables: 2

The number of figures: 6

The number of references: 75

The number of words in the *Abstract*: 249

The number of words in the *Introduction*: 749

The number of words in the *Discussion*: 1499

BPH-1: Benign prostatic hyperplasia epithelial cell line; CCND1: CyclinD1; CDK: Cyclin-dependent kinase; C_T: Threshold cycle values; c-MYC: V-myc myelocytomatosis viral oncogene homolog (avian); CTBP1: C-terminal binding protein 1; DU145: Prostate adenocarcinoma, brain metastatic site; EPHB2: EPH receptor B2; EZH2: Enhancer of zeste homolog 2; FBS: Fetal bovine serum; GSK-J4: KDM6 family selective inhibitor, Ethyl-3-(6-(4,5-dihydro-1H-benzo[d]azepin-3(2H)-yl)-2-(pyridin-2-yl)pyrimidin-4-ylamino)propanoate, GSK-J1 Pro-Drug, JHDM Inhibitor II Pro-Drug; H3K27me$_3$:Histone3 lysine27 tri-methylation; HKG: Housekeeping gene; KDM6A: Lysine demethylase 6A; KDM6B: Lysine demethylase 6B; LNCaP: Prostate adenocarcinoma, lymph node metastatic site; mPCa: Metastatic prostate cancer; MMP10: Matrix metallopeptidase 10 (stromelysin 2); MMP13: Matrix metallopeptidase 13 (collagenase 3); NF2: Neurofibromin 2 (merlin); PC3: Prostate adenocarcinoma, bone metastatic site; PCa: Prostate cancer; PLAUR: Plasminogen activator urokinase receptor; PTMs: Post translational modifications; pRb: Phosphorylated Retinoblastoma; RT-qPCR: Quantitative polymerase chain reaction; siRNA: small interfering RNA; VEGFA: Vascular endothelial growth factor A

ABSTRACT

Elevated expression of lysine demethylase 6A (KDM6A) and 6B (KDM6B) has been reported in prostate cancer (PCa). However, the mechanism underlying the specific role of KDM6A/B in PCa is still fragmentary. Here, we report novel KDM6A/B downstream targets involved in controlling PCa cell proliferation. KDM6A and KDM6B mRNAs were higher in LNCaP but not in PC3 and DU145 cells. Higher KDM6A mRNA was confirmed at the protein level. A metastasis associated gene focussed oligonucleotide array was performed to identify KDM6A/B dependent genes in LNCaP cells treated with a KDM6 family selective inhibitor, GSK-J4. This identified 5 genes (c-MYC, NF2, CTBP1, EPHB2, PLAUR) that were decreased more than 50 % by GSK-J4 and c-MYC was the most downregulated gene. Array data was validated by quantitative RT-PCR, which detected a reduction in c-MYC steady state mRNA and pre-spliced mRNA, indicative of transcriptional repression of c-MYC gene expression. Furthermore, c-MYC protein was also decreased by GSK-J4. Importantly, GSK-J4 reduced mRNA and protein levels of c-MYC target gene, CyclinD1 (CCND1). Silencing of KDM6A/B with siRNA confirmed that expression of both c-MYC and CCND1 are dependent on KDM6B. Phosphorylated Retinoblastoma (pRb), a marker of G1 to S-phase transition, was decreased by GSK-J4 and KDM6B silencing. GSK-J4 treatment resulted decrease in cell proliferation and cell number, detected by MTS assay and conventional cell counting, respectively. Consequently, we conclude that KDM6B controlling c-MYC, CCND1 and pRb contribute regulation of PCa cell proliferation, which represents KDM6B as a promising epigenetic target for the treatment of advanced PCa.

Key words: epigenetic regulation, KDM6A/B, c-MYC, proliferation, prostate cancer

SIGNIFICANCE STATEMENT

Lysine demethylase 6A (KDM6A) and 6B (KDM6B) were upregulated in prostate cancer (PCa). Here, we reported novel KDM6A/B downstream targets involved in controlling PCa cell proliferation. Amongst 84 metastasis associated genes, c-MYC was the most inhibited gene by KDM6 family inhibitor, GSK-J4. This was accompanied by decreased c-MYC target gene, CCND1 and pRb, which were selectively dependent on KDM6B. GSK-J4 decreased proliferation and cell counting. Consequently, we conclude that KDM6B controlling c-MYC, CCND1 and pRb contribute regulation of PCa proliferation.

4

INTRODUCTION

Prostate cancer (PCa) is the second leading cause of deaths and first most commonly diagnosed type of new cancer cases among men in US. Although localized PCa is potentially curable by surgery and radiotherapy, unfortunately metastatic PCa (mPCa) still remains untreatable. More dramatically, patients mortality increases within 2-3 years after transition to the lethal and aggressive stage of mPCa (Graça et al., 2016; Varambally et al., 2002) highlighting the need for further investigation on underlying mechanisms of metastasis to develop new therapeutic strategies.

PCa is a complex and heterogeneous disease arising through genetic and epigenetic alterations (Jerónimo et al., 2011; Vieira et al., 2014). In line with this, PCa is proposed as a model of "epigenetic catastrophe" due to occurrence of global or gene specific epigenetic changes at early stages of tumor development and throughout disease progression (Chinaranagari et al., 2015; He et al., 2013; Seligson et al., 2005). Post translational modifications (PTMs) of N-terminal histone tails are one of the main epigenetic regulatory mechanisms that is associated with activation or repression of gene expression due to modulation of DNA accessibility (Hess-Stumpp, 2005; Turner, 1993). A repressive histone mark, histone3 lysine27 tri-methylation (H3K27me$_3$) was found to be dysregulated in PCa (Ellinger et al., 2012; Ngollo et al., 2014) owing to change in expression or activity of key regulatory chromatin modifying enzymes including histone methyltransferase, EZH2 (enhancer of zeste homolog 2) and it's counter regulator Jumonji domain containing demethylases, KDM6A (lysine demethylase 6A, also known as UTX) and KDM6B (also known as JMJD3) (Daures et al., 2018; Daures et al., 2016). To date the expression of EZH2 (Daures et al., 2016; Ngollo et al., 2014; Varambally et al., 2002), its regulatory role in regulation of metastasis-associated gene expression (Shin and Kim, 2012) and the functional consequences of altered EZH2 expression on invasion, proliferation and metastasis of PCa has been widely studied (Chase and Cross, 2011; Karanikolas et al., 2010; Ngollo et al., 2017; Shin and Kim, 2012). In the case of KDM6A, it was found to be upregulated in PCa (Vieira et al., 2014) and reported as a PCa specific gene (Jung et al., 2016). KDM6B levels were also reported to be

5

elevated in mPCa with progression of disease severity (Xiang et al., 2007). KDM6B was proposed as a key regulator for determination of metastasis development due to presence of KDM6B expression into the nucleus of tumor cell lines implying that KDMs may act as a tumor suppressor or oncogenes (Daures et al., 2016). However, to our knowledge there is no study investigated the contribution of both KDM6A and KDM6B to the regulation of PCa metastatic features via modulation of metastasis-associated gene expression yet. In this context, to further investigate the functional importance of KDM6A and KDM6B in PCa (Hong et al., 2007), a selective pharmacological inhibitor, GSK-J4, which was designed as a pro-drug by using 3D structural prediction of the catalytic sites of KDM6A and KDM6B via addition of ethyl ester groups to the GSK-J1 to overcome the limited cellular permeability (Kruidenier et al., 2012), was used in this study.

The proto-oncogene c-MYC (V-myc myelocytomatosis viral oncogene homolog (avian)) encodes an important transcription factor, which is participated in initiation, growth and progression of tumors owing to its modulatory role on carcinogenesis related mechanisms including regulation of cell cycle and proliferation (Conacci-Sorrell and McAnulty, 2020; Elliott et al., 2019; Meškytė and Keskas, 2020; Venkateswaran, 2020). A number of studies conducted in human tissues revealed that mRNA levels of c-MYC is overexpressed in prostate adenocarcinomas compared to benign prostate hyperplasia (Buttyan et al., 1987; Dunn et al., 2006; Fleming et al., 1986; Tomlins et al., 2007). In transgenic mouse models, transient inactivation of c-MYC was found to be associated with maintained regression of tumors (Felsher and Bishop, 1999; Jain et al., 2002; Pelengaris et al., 1999). Therefore, inactivation of c-MYC might be proposed as a potential therapeutic target for treatment of PCa.

Initially, we aimed to investigate the role of KDM6A and KDM6B in transcriptional regulation of metastasis-associated genes in PCa metastatic cell line, LNCaP, in which levels of both enzymes were higher compared to BPH-1, and identified c-MYC as the most inhibited gene by GSK-J4. Owing to critical role of c-MYC in controlling proliferation, it is imperative to further investigate c-MYC contributed modulation of proliferation via regulation of its downstream target gene expression by KDM6A or KDM6B to identify underlined epigenetic mechanism in order to develop new therapeutic strategies for the treatment of elevated c-MYC involved diseases including PCa.

6

MATERIALS-METHODS

Materials

RPMI 1640 Medium, DMEM/F12, Penicillin-Streptomycin, L-Glutamine, Opti-MEM™ I Reduced Serum Medium were purchased from Gibco. QuantiTect Reverse Transcription Kit (205311) (Hilden; Germany), RNeasy Mini Kit (74104) (Hilden; Germany), RNase-Free DNase Set (79254) (Hilden; Germany), RT² Profiler™ PCR Array Human Tumor Metastasis (330231) (Maryland, USA), RT² SYBR Green PCR Master Mix (330504), RT² First Strand Kit (330401) (Maryland, USA) were all purchased from Qiagen. Silencer™ Select Negative Control No. 1 siRNA (4390843) (USA), KDM6A siRNA (s14736) (USA), KDM6B siRNA (s23109) (USA), Lipofectamine™ 2000 were obtained from Thermo Fisher. The LightCycler® 480 SYBR Green I Master (Mannheim, Germany) was obtained from Roche and CellTiter 96® AQ$_{ueous}$ One Solution Cell Proliferation Assay (G3582) purchased from Promega.

Cell Culture

All human prostate cell lines including BPH-1 (benign prostatic hyperplasia epithelial cell line), LNCaP (prostate *adenocarcinoma*, lymph node *metastatic* site), PC3 (prostate *adenocarcinoma*, bone *metastatic* site) and DU145 (prostate *adenocarcinoma*, brain *metastatic* site) were a kind gift from Prof. Petek Ballar (Ege University, PhD, Turkey). BPH-1 and LNCaP cell lines were cultured and propagated in 10 % FBS (fetal bovine serum), 1 % glutamine, 1 % penicillin and streptomycin supplemented RPMI-1640 media. PC3 and DU145 cell lines were routinely cultured and maintained in DMEM/F12 media containing 10 % FBS, 1 % glutamine, 1 % penicillin and streptomycin. Based on dose response and time course data presented in results section, LNCaP cells were treated with either DMSO (0.1 %) as a control or 30 μM GSK-J4 in 1 % FBS, 1 % glutamine, 1 % penicillin and streptomycin supplemented RPMI-1640 media for 18 hours.

RNA Isolation, Reverse Transcription, Quantitative Polymerase Chain Reaction (RT-qPCR)

Total RNA was isolated from at least three biological replicates of related cell lines by using RNeasy Mini Kit according to manufacturer's protocol and quantified by Nanovette (Beckman Coulter). 100 ng of RNA was reverse transcribed into cDNA by using QuantiTect Reverse Transcription Kit according to the manufacturer's instructions. cDNA samples were amplified using LightCycler$^®$ 480 SYBR Green I Master mix and the primer sets shown in Table 1 using a LightCycler$^®$ 480 Real-Time PCR System. Briefly, working solution was made up by mixing 10 µl The LightCycler® 480 SYBR Green I Master mix, 0.8 µl forward-reverse primer mixture (to make final concentration 0.5 µM) and 8.2 µl RNase-free water per sample. Lastly, 19 µl reaction mix was loaded into each well of 96-well plates followed by addition of 1 µl cDNA sample and RNase-free water as a blank. The reaction was carried out according to following protocol: Pre-incubation 95°C 5 minutes (1 cycle), PCR Cycling 95°C 20 seconds, 62°C 20 seconds, 72°C 20 seconds (45 cycle), Melt Curve 95°C 5 seconds, 65°C 1 minute, 97°C continuous (1 cycle), cooling 40°C 30 seconds (1 cycle). PCR data was normalized to total RNA concentration. In this study, fold change of each gene is calculated using $2^{(-\Delta\Delta C_T)}$ method, which is widely used to analyse the relative changes in gene expression from RT-qPCR experiment. The C_T (cycle threshold) values mainly represent the number of cycles, where the PCR amplification curve cross the threshold. Based on this formula, following calculation of $\Delta\Delta C_T$ values (ΔC_T (GSK-J4 sample)- ΔC_T (DMSO sample), fold change is calculated using $2^{(-\Delta\Delta C_T)}$ formula due to exponential nature of PCR. Basically, for GSK-J4 treated sample, the result of $2^{(-\Delta\Delta CT)}$ calculations mainly shows the fold change in expression of gene of interest relative to untreated control sample, DMSO.

Human Tumor Metastasis PCR Array

Total RNA samples for PCR Array were extracted from three biological replicates of cells with an additional on-column DNAse digestion step and those samples, which passed the stringent quality and purity criteria (sample concentration should be at least 40 µg/mL, A_{260}:A_{230} ratio>1.7 and A_{260}:A_{280} should be 1.8-2), were reverse transcribed (400 ng, genomic DNA eliminated) by using RT² First Strand Kit according to manufacturer's instructions. Briefly, samples were subjected to RT² Profiler™ PCR Array Human Tumor Metastasis, which profiles 84 tumor metastasis genes involve in diverse

8

functions including regulation of cell cycle, cell growth and apoptosis as well as cell adhesion molecules, extracellular matrix molecules and transcription factors. The amplification reaction was carried out in 96 well plate format in LightCycler® 480 Real-Time PCR System based on the following protocol: heat activation: 95°C 10 minutes (1 cycle), PCR cycling: 95°C 15 seconds followed by 60°C 1 minute (45 cycles), melt curve: 60°C 15 seconds and 95°C continuous (1 cycle) and the threshold cycle values (C_T) were analysed by using web based SABiosciences PCR Array Data Analysis Software[1] (Yildirim-Buharalioglu et al., 2017). Normalisation analyses was performed by automatic selection of RPLP0 as a housekeeping gene (HKG) amongst 5 HKG included in the array due to its most stable expression profile across the samples and changes were calculated by using manufacturer's software, which produce mean fold change and *p* values after false discovery rate correction.

Western Blotting

Cells were lysed in SDS lysis buffer (2 % SDS (w/v), 16 % glycerol (v/v) and 50 mM Tris, pH 6.8) and concentration of total protein samples were measured using BCA™ Protein Assay Kit (Thermo) (Smith et al., 1985). Equal amounts of reduced and denatured protein were loaded into SDS-polyacrylamide gels to fractionate by using gel electrophoresis and transferred to PVDF membranes (Biorad). Blots were blocked in 5 % skimmed milk prepared in TBS-T, membranes were incubated in primary antibodies overnight at 4°C followed by incubation with appropriate HRP-conjugated secondary antibodies at room temperature. Clarity Western ECL Substrate (Biorad) was used to detect proteins in Fusion FX7 (Vilber Lourmat) and protein bands were quantified by ImageJ software. The antibodies used were KDM6A (1/1000 dilution) (Yildirim-Buharalioglu et al., 2017), c-MYC (1/500 dilution) (Du et al., 2020), CCND1 (1/500 dilution) (Zhang et al., 2020), Phospho-Rb (Ser807/811) (1/1000 dilution) (Yildirim-Buharalioglu et al., 2017) (Cell Signaling), Histone H3 (Abcam) (1/1000

---

[1] https://dataanalysis.qiagen.com/pcr/arrayanalysis.php

dilution) (Yildirim-Buharalioglu et al., 2017), H3K27me3 (Diagenode) (1/1000 dilution) (Abe et al., 2020), GAPDH (Millipore) (1/10000 dilution) (Yildirim-Buharalioglu et al., 2017).

siRNA Mediated Silencing of KDM6A or KDM6B

One day before transfection 6×10^4 LNCaP cells were plated in 24 well plates and incubated overnight. Subsequently, LNCaP cells were transfected with 20 pmol of each individual siRNA for 72 hours by using Lipofectamine 2000 Transfection Reagent according to manufacturer's protocol. *Silencer* ™ Select Negative Control No.1 (Ambion), KDM6A directed siRNA (si oligo ID: s14736, Ambion, 5' GCAUUGUGAAAGUAAUAGAtt 3'), KDM6B directed siRNA (si oligo ID: s23109, Ambion, 5' UCCUGUUCGUGACAAGUGAtt 3').

Cell Proliferation

Proliferation of LNCaP cells were established by quantitative colorimetric assay and conventional cell counting. For MTS cell proliferation assay, cells were cultured at 7×10^3 cells per well in 96 well plates and incubated overnight. Briefly, cells were treated with GSK-J4 for 18 hours. Subsequently, CellTiter 96® AQ$_{ueous}$ One Solution Reagent (Promega) (He et al., 2013) containing tetrazolium compound, MTS, was added according to manufacturer's protocol and incubated for further 3 hours at 5 % CO_2 and 37°C incubator. Absorbance was read at 490 nm in Varioskan Flash (Thermo Scientific) and average absorbance readings of blank wells (no cell) were subtracted from all other absorbance values in order to generate corrected readings. Absorbance values of this assay were obtained from three independent experiments with triplicate technical replication for each assay. For conventional haemocytometer counting, briefly LNCaP cells were cultured as described above, washed with warm DPBS, trypsinized and proceeded with cell counting utilizing Trypan blue exclusion (Morten et al., 2016).

Statistics

GraphPad Prism 9.2.0 is used to perform statistical analysis. Shapiro-Wilk test was used to check whether data sets were normally distributed. Two tail unpaired t-test or for multiple comparisons, one-way ANOVA with Dunnett's multiple comparisons or two-way ANOVA with Bonferroni's multiple comparisons (just for data in Figure 3) tests were used to analyse means of normally distributed data. Graphs with plus and minus FBS present two variables, but these were conducted as separate experiments and one-way ANOVA was performed for – and + FBS separately. However, we merged them together to plot in a single graph in the interest of space being concise. All data in this manuscript presented as mean values ± standard deviation (S.D.) of at least three independent experiments, unless otherwise stated. * indicates $p < 0.05$, ** indicates $p < 0.01$, *** indicates $p < 0.001$.

RESULTS

Changes in Constitutive KDM6A and KDM6B Levels in PCa Metastatic Cell Lines Compared to BPH-1

To investigate whether KDM6A or KDM6B enzymes contribute to epigenetic regulation of metastasis-associated genes in human PCa, at first we measured changes in constitutive KDM6A and KDM6B mRNA, protein levels by qRT-PCR and Western Blotting, respectively in untreated human metastatic prostate cancer cell lines including LNCaP, PC3, DU145 compared to BPH-1. Our data shown in Figure 1A demonstrated that steady state mRNA levels of KDM6A were higher in LNCaP cells (17.7 fold; lower-upper 95 % Confidence Interval (CI) -1.95-37.34; p=0.0022) but no changes in either PC3 or DU145 cells compared to BPH-1. Moreover, mRNA levels of KDM6B were higher in LNCaP cells (3.1 fold; 95 % CI 1.23-4.96; p=0.0007), whereas there was no change in PC3 or DU145 cells compared to BPH-1 (Figure 1B). 36B4 mRNA levels were not changed in any of these metastatic cell lines (Figure 1C). To determine whether observed alterations at mRNA levels of KDM6A and KDM6B were reflected in changes in protein levels, Western blotting was performed. However, due to the lack of commercially available good quality antibodies we tried for KDM6B we were not able to obtain protein data for KDM6B. There was no detectable KDM6A protein expression in BPH-1 cells. KDM6A protein level was higher in LNCaP cells (1.07 fold; 95 % CI 0.45-1.69; p<0.0001) but not in PC3 and DU145 cells compared to BPH-1 (Figure 1D), which was in consistent with KDM6A mRNA data (Figure 1A). Our data provided in Figure 1 showed that LNCaP is the only metastatic cell line in

12

which both constitutive KDM6A and KDM6B mRNA and protein levels were higher compared to BPH-1. Hence, these data led us to question whether KDM6A/B contributes transcriptional regulation of metastasis involved genes in LNCaP cells.

Optimization of Inhibition by KDM6 Family Selective Inhibitor, GSK-J4 in LNCaP Cell Line

Optimization of KDM6 inhibition by GSK-J4 was accomplished by following two strategies including, measuring the changes in global H3K27me$_3$ levels and mRNA levels of known KDM6A, KDM6B and GSK-J4 regulated genes (MYB, CCND1, SLC4A4) from previous studies (Benyoucef et al., 2016; Daures et al., 2018) (for CCND1 our data obtained from human monocyte derived macrophages not shown, preparing the manuscript), in dose response and time course samples of GSK-J4 treated LNCaP cells. Because cell permeable pro-drug GSK-J4 (Kruidenier et al., 2012) needs to be hydrolysed by esterases, which might present also in serum, in our study we also investigated the impact of diverse serum concentration supplemented in culture medium on GSK-J4 potency.

Although there was a trend towards increase in global H3K27me$_3$ levels in response to 10 µM (Das et al., 2017; Mandal et al., 2017) and 30 µM (Kruidenier et al., 2012) but not 4 µM (Morozov et al., 2017; Sui et al., 2017) GSK-J4 applied both in FBS free and 1 % FBS supplemented medium, the data was not clear enough to determine the appropriate dose and serum condition (Figure 2A). To verify the activity of our GSK-J4, we validated inhibition of KDM6A, KDM6B and GSK-J4 regulated genes MYB (Benyoucef et al., 2016), CCND1 (our data obtained from human monocyte derived macrophages not shown, preparing the manuscript) and SLC4A4 (Daures et al., 2018), respectively in our preparations of LNCaP cells. Relative CCND1 mRNA level was decreased 43 % (95 % CI 3.6-81.4; p=0.033) by 10 µM GSK-J4 in 1 % FBS supplemented medium. Although there was a fall in CCND1 mRNA levels by 60 % (95 % CI 32-88; p=0.0008) in response to 30 µM GSK-J4 in FBS free medium, the most dramatic inhibition in CCND1 transcriptional level occurred at 30 µM GSK-J4 in 1 % FBS supplemented medium by 70 % (95 % CI 31-108; p=0.0021) (Figure 2B). 30 µM GSK-J4 treatments in FBS free and 1 % FBS contained medium displayed similar decreases in SLC4A4 mRNA levels by 57 (95 % CI 37.5-75.5; p<0.0001) and 58 % (95 % CI 16-99; p=0.010), respectively

(Figure 2C). 10 μM and 30 μM GSK-J4 treated in culture medium without FBS down-regulated MYB mRNA levels by 32 (95 % CI 5.8-57.2; p=0.019) and 67 % (95 % CI 40.8-92.2; p=0.0002), respectively. On the other hand, there was falls at MYB mRNA levels by 52 (95 % CI 26.8-76.2; p=0.0008) and 56 % (95 % CI 30-79.5; p=0.0006) in response to 10 μM and 30 μM GSK-J4 treatment in serum supplemented medium (Figure 2D). 36B4 mRNA level was not changed (Figure 2E). In outline, 30 μM GSK-J4 prepared 1 % FBS supplemented medium resulted in over 50 % inhibition in mRNA levels of all three positive control genes (Figure 2B-C-D). Hence, for time course experiment LNCaP cells were treated with 30 μM GSK-J4 prepared in 1 % FBS supplemented medium for 6, 18, 24 and 48 hours.

Although there was a trend towards minor accumulation of global H3K27me$_3$ levels at 18 hours of GSK-J4 treatment (Figure 3A), the data needs to be further investigated by measuring change in CCND1, SLC4A4 and MYB mRNA levels in prepared time course samples of GSK-J4. Strikingly, CCND1 mRNA level was decreased to the similar extent at 6 hours (68 %; 95 % CI 47-89; p<0.0001) and 18 hours (67 %; 95 % CI 46-87; p<0.0001) and the inhibitory effect was maintained up to 48 hours (49 %; 95 % CI 28-70; p<0.0001) (Figure 3B). Expression of SLC4A4 was inhibited within 6 hours (47 %; 95 % CI 26-67; p<0.0001) and reached its minimum at 18 hours (57 %; 95 % CI 36-77; p<0.0001). Furthermore, the inhibitory effect on expression profile was still statistically significant at 24 (35 %, 95 % CI 14-55; p=0.0009) and 48 (34 %; 95 % CI 13-55; p=0.0011) hours to the similar extent (Figure 3C). In the case of MYB, it was down-regulated by 51 (95 % CI 26-76, p=0.0001), 66 (95 % CI 41-90; p<0.0001, 68 (95 % CI 43-92; p<0.0001) and 71 (95 % CI 46-95; p<0.0001) % with prolonged exposure to GSK-J4 (Figure 3D). 36B4 mRNA level was not changed under any of these experimental conditions (Figure 3E). Overall, the decision was taken to use 30 μM GSK-J4 for 18 hours in 1 % FBS supplemented medium for further experiments.

Inhibitory Effect of GSK-J4 on mRNA Profiling of Human Tumor Metastasis Genes

Metastasis-associated genes, whose expression are regulated by KDM6A or KDM6B, were profiled using a commercially available Human Tumor Metastasis RT² Profiler PCR Array, which is comprised

14

of 84 genes known to be implicated in metastasis, by using GSK-J4 in highly invasive PCa cell line, LNCaP owing to higher KDM6A and KDM6B levels compared to BPH-1 (Figure 1). Accordingly, data presented in Table 2 and Figure 4A, steady state mRNA levels of 9 genes out of 84 were altered greater than 2-fold by GSK-J4 in LNCaP cells. Amongst those 9 genes, of which 5 (c-MYC, NF2, CTBP1, EPHB2, PLAUR) shown in bold in Table 2 were down-regulated, whereas levels of 4 were increased in response to GSK-J4. As explained in introduction, GSK-J4 selectively inhibits KDM6 family demethylases, KDM6A and KDM6B, which mediate demethylation of repressive H3K27me$_3$ epigenetic marker, resulting in activation of gene expression. Hence, to identify possible targets for KDM6A and KDM6B we focussed on GSK-J4 down-regulated genes, of which all were functionally associated with regulation of cell growth and proliferation. Strikingly, it was revealed that c-MYC is the most highly down-regulated gene (73 %; 95 % CI 49-98; p=0.0011) in our list of GSK-J4 decreased genes, which strongly suggests that c-MYC is the primary target of GSK-J4 for the regulation of LNCaP cell proliferation.

Validation of array data for c-MYC expression in KDM6A/B silenced LNCaP cells pharmacologically

To confirm our PCR array data on c-MYC expression, initially c-MYC mRNA levels were quantified in GSK-J4 treated cells by qRT-PCR. Moreover, to investigate whether decreased c-MYC expression by GSK-J4 was due to inhibition of transcription, we measured change in c-MYC pre-spliced mRNA level, which is a surrogate marker of transcriptional rate (Elferink and Reiners, 1996). As it is well known, steady state mRNA levels is mainly determined by two parameters rate of synthesis (also known as rate of transcription) and rate of degradation (Hao and Baltimore, 2009). Therefore, change in steady state mRNA level does not necessarily reflect change in rate of transcription. For this reason, we measured pre-spliced mRNA level, which is also named as nascent (un-spliced) chromatin associated transcripts in a previous study (De Santa et al., 2009). Our data showed that steady state mRNA level of c-MYC was decreased by 77 % (95 % CI 59-94; p=0.0003) in response to GSK-J4 (Figure 4B), which confirmed the PCR array data (Table 2, Figure 4A). Furthermore, GSK-J4 treatment resulted in 52 % (95 % CI 30-73; p=0.0228) decrease in pre-spliced c-MYC mRNA levels

15

(Figure 4B), which displayed quite similar pattern with inhibition of c-MYC mRNA by GSK-J4. Thus, our data strongly suggests that observed change at c-MYC mRNA level was at least partially due to changes in transcriptional rate. To verify the effect on protein level, change in c-MYC protein level was measured by Western blotting in GSK-J4 treated LNCaP cells (Figure 4C). c-MYC protein level was down-regulated by 75 % (95 % CI 25-124; p=0.0144) after GSK-J4, which is consistent with the inhibitory effect on steady state mRNA level.

Regulation of c-MYC expression is selectively dependent on KDM6B in LNCaP cells

Because GSK-J4 is a KDM6 family selective inhibitor, the regulatory role of KDM6A and KDM6B on c-MYC expression was investigated by siRNA mediated silencing of KDM6A, KDM6B or both. Silencing of KDM6A or KDM6B was compared to non-targeting negative control siRNA and as housekeeping gene change in 36B4 mRNA levels was also measured for further control. The ability of siKDM6A or siKDM6B to effectively silence KDM6A and KDM6B mRNA levels was validated by measuring change in KDM6A and KDM6B mRNA levels by qRT-PCR. As shown in Figure 5A, KDM6A mRNA level was downregulated by siRNA mediated silencing of KDM6A alone and in combination with KDM6B by 62 (95 % CI 41-83; p<0.0001) and 67 % (95 % CI 46-87; p<0.0001), respectively, whereas siKDM6B transfection did not have inhibitory effect on KDM6A mRNA level, as expected. Furthermore, KDM6B mRNA level was decreased by siRNA mediated silencing of KDM6B and in combination with KDM6A by 57 (95 % CI 28-86; p=0.0013) and 63 % (95 % CI 33-92; P=0.0007), respectively (Figure 5A). Not surprisingly, mRNA levels of KDM6B were not affected by siRNA mediated silencing of KDM6A (Figure 5A). Moreover, 36B4 mRNA level was not changed under any of these experimental conditions (Figure 5D). Accordingly, the data presented in Figure 5A, KDM6A and KDM6B silencing was selective. Specificity was verified by measuring change in KDM6A protein level (Figure 5B), whereas data for KDM6B could not be provided due to no available good quality antibody we tried against KDM6B. siRNA mediated silencing of KDM6A alone and together with KDM6B decreased KDM6A protein level by 80 (95 % CI 10-150; p=0.026) and 75 % (95 % CI 5-144; p=0.036), respectively, which is consistent with the effect on mRNA data, whereas there was no inhibitory effect of siRNA mediated silencing of KDM6B on KDM6A protein

16

level, as anticipated (Figure 5B). siKDM6A transfection did not effect on c-MYC mRNA levels. However, siRNA mediated silencing of KDM6B alone and in combination with KDM6A down-regulated c-MYC mRNA level by 37 (95 % CI 22-52; p=0.0003) and 24 (95 % CI 9.3-38.7; p=0.004) %, respectively (Figure 5C), which demonstrated that c-MYC expression is selectively dependent on KDM6B. Supporting this data, a pilot protein study (Figure 5E) suggested that there was a tendency towards decrease in c-MYC protein levels with silencing of KDM6B alone and together with KDM6A.

Decline in expression of downstream targets of c-MYC was concomitant with decreased proliferation of LNCaP cells

To further investigate the downstream mechanism of KDM6 dependent c-MYC controlling proliferation of LNCaP cells, firstly change in mRNA and protein levels of CCND1, which is involved, with c-MYC, in a major proliferation-control pathway (Daksis et al., 1994; Perez-Roger et al., 1999), was measured by qRT-PCR and Western blotting, respectively in KDM6A/B silenced cells pharmacologically or with siRNA. In consistent with the inhibitory effect on mRNA level (Figure 2B, 3B), CCND1 protein level was profoundly decreased by 86 % (95 % CI 68-103; p=0.0002) in response to GSK-J4 (Figure 6A). Furthermore, CCND1 mRNA level was decreased by siRNA mediated silencing of KDM6B alone and together with KDM6A by 30 (95 % CI 6.4-53.6; p=0.016) and 48 (95 % CI 24-72; p=0.001) %, recpectively, which revealed that CCND1 mRNA expression selectively depends on KDM6B (Figure 6B). Secondly, pRb protein level, which is a negative marker of cell cycle progression, was decreased 72 % (95 % CI 55-88; p=0.0003) by GSK-J4 (Figure 6C). Moreover, siRNA mediated silencing of KDM6B alone and together with KDM6A down-regulated pRb protein level by 48 (95 %CI 6-89; p=0.0282) and 51 (95 % CI 9-92; p=0.0213) % respectively (Figure 6D), implying that KDM6B dependent pRb regulation may involve in inhibition of LNCaP cell proliferation.

Functionally, effect of GSK-J4 on proliferation of LNCaP cells was assessed by CellTiter 96® AQ$_{ueous}$ One Solution Cell Proliferation Assay (Promega) and counting of total number of cells using

17

conventional haemocytometer. According to data from cell proliferation assay, LNCaP proliferation

was decreased by 37 % (95 % CI 28-46, p<0.0001) after 18 hours of GSK-J4 treatment (Figure 6E).

Supporting this finding, there was a 30 % (95 % CI 25-34; p<0.0001) decrease in total number of cells

in GSK-J4 treated cells compared to DMSO (Figure 6F). However, to further investigate whether

observed decrease in cell number is due to increase in cell death or reduction in proliferation by GSK-

J4, we also measured change in percentage of Trypan blue positive cells (Figure 6G), which reflects

cell death, in GSK-J4 treated cells versus DMSO. According to data in Figure 6G, there was no

change in percentage of trypan blue positive cells after GSK-J4 compared to DMSO, which supports

that observed decrease in total cell number is mainly due to decreased proliferation rather than

elevated cell death by GSK-J4 in LNCaP cells. Taken together, decline in levels of c-MYC

downstream target genes CCND1 and pRb by GSK-J4 were concomitant with decreased proliferation

of LNCaP cells.

DISCUSSION

PCa, the second leading cause of cancer related mortality arises from acquired genetic and epigenetic

alterations (Ellinger et al., 2012; Ngollo et al., 2014; Shukeir et al., 2006; Wu et al., 2015). However,

unlike genetic alterations epigenetic changes are reversible processes regulated by pharmacologically

targetable histone modifying enzymes. Altered PTMs of histones have been found to be implicated in

PCa development and progression (Bianco-Miotto et al., 2010; Ke et al., 2009; Seligson et al., 2005),

owing to impaired expression or activity of key chromatin modifying enzymes (Miremadi et al.,

2007). Previous study conducted in PCa patient tissues reported that KDM6A is a PCa specific gene

due to its potential role during transition from high grade prostatic intraepithelial neoplasia to PCa

(Jung et al., 2016). Although limited levels of KDM6B protein was detected in benign prostate, it was

higher in PCa and the increase was even greater in mPCa. Moreover, KDM6B levels were found to be

correlated with disease progression (Xiang et al., 2007). Therefore, to clarify the oncogenic role of

KDM6A/B in PCa, initially we measured change in KDM6A and KDM6B levels in LNCaP, PC3,

DU145 cells compared to BPH-1. Strikingly, KDM6A and KDM6B mRNA levels were remarkably

higher in androgen receptor (AR) positive LNCaP cells but not in AR negative DU145 and PC3 cells

(Figure 1A-B), implying a AR-dependent involvement of both enzymes which is also suggested by previous studies for KDM6B (Daures et al., 2016; Morozov et al., 2017) but no data has been reported for KDM6A yet. It is crucial to further investigate the role of both enzymes in AR signalling but this is not the scope of this manuscript. Increased mRNA levels of KDM6A and KDM6B were confirmed by individual studies, which were reported elevated KDM6A in human PCa tissues (Vieira et al., 2014) and KDM6B in LNCaP cells versus PWR-1E (Daures et al., 2016). However, to our knowledge consistent with mRNA data, a profound KDM6A protein expression (Figure 1D) detected for the first time in LNCaP cells with our study, which supported our proposal that KDM6A may also involve in modulation of metastasis in PCa, whereas the expression was not even detectable in BPH-1 cells. Therefore, to further investigate underlying mechanisms of our hypothesis we used GSK-J4, which is suggested as a potential therapeutic option for treatment of acute lymphoblastic leukaemia (Ntziachristos et al., 2014) and brainstem glioma (Hashizume et al., 2014). According to data to optimize inhibition of KDM6A/B with GSK-J4 (Figure 2-3), there was no clear accumulation in total $H3K27me_3$, which is consistent with previous study showed that GSK-J4 promoted elevated $H3K27me_3$ in the specific promoters regions of KDM6A/B regulated genes rather than global change in levels of this modification (Ntziachristos et al., 2014). Therefore, the activity of GSK-J4 was confirmed by measuring decrease in expression of KDM6A, KDM6B and GSK-J4 regulated genes MYB (Benyoucef et al., 2016), CCND1 (preparing the manuscript) and SLC4A4 (Daures et al., 2018), respectively.

To identify KDM6A/B regulated metastasis-associated genes, mRNA levels were profiled by performing Human Tumor Metastasis RT² Profiler PCR Array in GSK-J4 treated LNCaP cells in which levels of both enzymes were higher. Analysis of metastasis array showed that 5 (c-MYC, NF2, CTBP1, EPHB2, PLAUR) out of 84 genes were down-regulated by GSK-J4 and strikingly all those genes were functionally tagged with regulation of cell growth and proliferation (Table 2, Figure 4A). In accordance with this, Jumonji C-domain containing KDMs were mainly found to be involved in regulation of proliferation in PCa cells in a genome wide study carried out to investigate the functional importance of 615 epigenetic players in PCa (Bjorkman et al., 2012). Recent studies demonstrated

19

regulatory roles of KDMs including KDM4B via controlling Wnt/β-catenin signaling (Sha et al., 2020) and KDM4C owing to activation of c-MYC and AKT (Lin et al., 2019) in PCa proliferation. KDM3A was reported to be participated in controlling PCa cell growth via modulatory role on c-MYC expression (Fan et al., 2016). Silencing of KDM6B was found to be implicated in decreased proliferation of multiple myeloma cells via modulation of MAPK signalling (Ohguchi et al., 2017). GSK-J4 resulted in decreased proliferation in glioma (Sui et al., 2017) and PC3 cells (Morozov et al., 2017). However, the underlying mechanism of KDM6A/B controlling proliferation of PCa cells regarding downstream targets has been incompletely understood. Therefore, we focused on KDM6A/B controlling regulation of c-MYC, which came up on top of our array as the most inhibited gene by GSK-J4 (Table 2, Figure 4A) and has been linked to PCa progression owing to its overexpression in PCa cell lines and patient tissues (Iwata et al., 2010; Pan et al., 2018; Rebello et al., 2017). Array data on c-MYC was verified by measuring change in steady state and pre-spliced mRNA levels (Figure 4B), which strongly suggested that observed inhibitory effect on c-MYC levels is at least partially due to inhibition of transcription by GSK-J4. The inhibitory effect by GSK-J4 is also verified at c-MYC protein level (Figure 4C) and c-MYC expression was found to be dependent on KDM6B that is also supported by a pilot protein study (Figure 5C-E). To test whether KDM6B regulates c-MYC in a direct manner, change in $H3K27me_3$ levels and KDM6B binding in the promoter of c-MYC could be further investigated by Chromatin Immunoprecipitation.

Owing to master regulator role of c-MYC in modulation of cell cycle and proliferation (Dang, 2012), we searched for the role of KDM6A/B in regulation of c-MYC downstream genes involve in controlling transition from G_0 to S phase of cell cycle. In the context of cell cycle regulation, transition from G_0 to G_1 is mainly achieved by activities of cyclin-dependent kinase (CDK) complexes such as Cyclin D (CCND)-CDK4-6. Therefore, as a c-MYC regulated cell cycle controlling gene, we demonstrated decreased mRNA and protein levels of CCND1 by GSK-J4 (Figure 2B, Figure 3B, Figure 6A) and with siRNA mediated silencing of KDM6B (Figure 6B). Supporting our data, CCND1 was found to be regulated by KDM6B in a direct manner via $H3K27me_3$ demethylase activity in PC3 cells, which was linked to progression of PCa (Cao et al., 2021). Although CCND1 is a known c-MYC

target gene, c-MYC controlling CCND1 expression was reported as controversial due to stimulatory (Daksis et al., 1994; Perez-Roger et al., 1999; Yu et al., 2005) or repressive (Philipp et al., 1994; Solomon et al., 1995) effects of c-MYC on CCND1, which seems to depend on specific stimuli and cell type. Because there is a strong positive correlation between c-MYC and CCND1 expression due to decrease in expression of both genes by GSK-J4, our study suggested that c-MYC is stimulatory on CCND1 expression in LNCaP cells.

In complex with CDK4-6, D type Cyclins are responsible for phosphorylation of Rb, which is negative regulator of cell cycle that is responsible for G_1 checkpoint control (García-Gutiérrez et al., 2019; Mateyak et al., 1999). Alterations in Rb signalling were reported in 25-50 % of prostatic adenocarcinomas and Rb depletion resulted in impaired cellular response to treatment in PCa cells, which strongly suggested that Rb status could be considered as a potential marker for modulation of therapeutic effectiveness (Sharma et al., 2007). Therefore, we thought as a downstream target of c-MYC it is crucial to identify KDM6A/B mediated regulation of Rb status in PCa. In line with this objective, decreased pRb protein by GSK-J4 and siRNA mediated silencing of KDM6A/B showed that pRb protein is selectively dependent on KDM6B (Figure 6C-D). Supporting our data, KDM6B mediated demethylation of Rb was found to be resulted in altered pRb due to repressed binding of CDK4 to Rb that is implicated in reduced pRb in embryonic tissue cells (Zhao et al., 2015). On the other hand, UTX mediated Rb transcription was found to play crucial role in UTX controlling mammalian primary cell growth (Terashima et al., 2010). Collectively, our and previous studies suggested that, regulation of Rb status by KDM6s seems to be cell type specific.

When Rb is hypo-phosphorylated, it physically interacts with S phase transcription factor E2F, which is implicated in repressed E2F regulated gene expression that is required for cell cycle progression and DNA replication (Giacinti and Giordano, 2006; Topacio et al., 2019). As a result of decreased c-MYC, CCND1 and pRb levels, proliferation of LNCaP cells were shown to be decreased by GSK-J4, which was demonstrated by following two different methods including measuring decrease in metabolic activity that is directly proportional of number of living cells and counting of total number of cells concomitant with no change in percentage of trypan blue positive cells (Figure 6E-G), which supports

21

that observed decrease in total cell number is mainly due to decreased proliferation rather than elevated cell death by GSK-J4 in LNCaP cells. To our knowledge, in consistent with our data inhibitory effect of GSK-J4 on PCa cell proliferation has been determined by limited number of studies (Cao et al., 2021; Morozov et al., 2017) but this is the first study, which shows the mechanism of KDM6s controlling proliferation of LNCaP cells via identifying KDM6B downstream targets c-MYC, CCND1 and pRb.

In conclusion, our data revealed that KDM6B controlling c-MYC, CCND1 and pRb contribute regulation of PCa cell proliferation that represents KDM6B as a promising epigenetic target for the treatment of advanced PCa.

AUTHORSHIP CONTRIBUTIONS

Designed research: Yıldırım-Buharalıoğlu

Conducted experiments: Yıldırım-Buharalıoğlu

Contributed new reagents or analytic tools: Yıldırım-Buharalıoğlu

Performed data analysis: Yıldırım-Buharalıoğlu

Wrote the manuscript: Yıldırım-Buharalıoğlu

REFERENCES

Abe S, Nagatomo H, Sasaki H and Ishiuchi T (2020) A histone H3.3K36M mutation in mice causes an imbalance of histone modifications and defects in chondrocyte differentiation.1-12.

Benyoucef A, Palii CG, Wang C, Porter CJ, Chu A, Dai F, Tremblay V, Rakopoulos P, Singh K, Huang S, Pflumio F, Hebert J, Couture JF, Perkins TJ, Ge K, Dilworth FJ and Brand M (2016) UTX inhibition as selective epigenetic therapy against TAL1-driven T-cell acute lymphoblastic leukemia. *Genes Dev* **30**:508-521.

Bianco-Miotto T, Chiam K, Buchanan G, Jindal S, Day TK, Thomas M, Pickering MA, O'Loughlin MA, Ryan NK, Raymond WA, Horvath LG, Kench JG, Stricker PD, Marshall VR, Sutherland RL, Henshall SM, Gerald WL, Scher HI, Risbridger GP, Clements JA, Butler LM, Tilley WD, Horsfall DJ and Ricciardelli C (2010) Global levels of specific histone modifications and an

epigenetic gene signature predict prostate cancer progression and development. Cancer epidemiology, biomarkers & prevention : a publication of the American Association for Cancer Research, cosponsored by the American Society of Preventive Oncology **19**:2611-2622.

Bjorkman M, Ostling P, Harma V, Virtanen J, Mpindi JP, Rantala J, Mirtti T, Vesterinen T, Lundin M, Sankila A, Rannikko A, Kaivanto E, Kohonen P, Kallioniemi O and Nees M (2012) Systematic knockdown of epigenetic enzymes identifies a novel histone demethylase PHF8 overexpressed in prostate cancer with an impact on cell proliferation, migration and invasion. *Oncogene* **31**:3444-3456.

Buttyan R, Sawczuk IS, Benson MC, Siegal JD and Olsson CA (1987) Enhanced expression of the c-myc protooncogene in high-grade human prostate cancers. *The Prostate* **11**:327-337.

Cao Z, Shi X, Tian F, Fang Y and Wu JB (2021) KDM6B is an androgen regulated gene and plays oncogenic roles by demethylating H3K27me3 at cyclin D1 promoter in prostate cancer. **12**:2.

Chase A and Cross NC (2011) Aberrations of EZH2 in cancer. *Clinical cancer research : an official journal of the American Association for Cancer Research* **17**:2613-2618.

Chinaranagari S, Sharma P, Bowen NJ and Chaudhary J (2015) Prostate cancer epigenome. *Methods in molecular biology (Clifton, NJ)* **1238**:125-140.

Conacci-Sorrell M and McAnulty J (2020) The Molecular 'Myc-anisms' Behind Myc-Driven Tumorigenesis and the Relevant Myc-Directed Therapeutics. *Small GTPases* **21**.

Daksis JI, Lu RY, Facchini LM, Marhin WW and Penn LJ (1994) Myc induces cyclin D1 expression in the absence of de novo protein synthesis and links mitogen-stimulated signal transduction to the cell cycle. *Oncogene* **9**:3635-3645.

Dang CV (2012) MYC on the path to cancer. *Cell* **149**:22-35.

Das A, Arifuzzaman S, Yoon T, Kim SH and Chai JC (2017) RNA sequencing reveals resistance of TLR4 ligand-activated microglial cells to inflammation mediated by the selective jumonji H3K27 demethylase inhibitor. **7**:6554.

Daures M, Idrissou M, Judes G, Rifai K, Penault-Llorca F, Bignon YJ, Guy L and Bernard-Gallon D (2018) A new metabolic gene signature in prostate cancer regulated by JMJD3 and EZH2. *Oncotarget* **9**:23413-23425.

Daures M, Ngollo M, Judes G, Rifai K, Kemeny JL, Penault-Llorca F, Bignon YJ, Guy L and Bernard-Gallon D (2016) The JMJD3 Histone Demethylase and the EZH2 Histone Methyltransferase in Prostate Cancer. *Omics : a journal of integrative biology* **20**:123-125.

De Santa F, Narang V, Yap ZH, Tusi BK, Burgold T, Austenaa L, Bucci G, Caganova M, Notarbartolo S, Casola S, Testa G, Sung WK, Wei CL and Natoli G (2009) Jmjd3 contributes to the control of gene expression in LPS-activated macrophages. *The EMBO journal* **28**:3341-3352.

Du J, Zhang G, Qiu H, Yu H and Yuan W (2020) A novel positive feedback loop of linc02042 and c-Myc mediated by YBX1 promotes tumorigenesis and metastasis in esophageal squamous cell carcinoma. **20**:75.

Dunn TA, Chen S, Faith DA, Hicks JL, Platz EA, Chen Y, Ewing CM, Sauvageot J, Isaacs WB, De Marzo AM and Luo J (2006) A novel role of myosin VI in human prostate cancer. *The American journal of pathology* **169**:1843-1854.

Elferink CJ and Reiners JJ, Jr. (1996) Quantitative RT-PCR on CYP1A1 heterogeneous nuclear RNA: a surrogate for the in vitro transcription run-on assay. *BioTechniques* **20**:470-477.

Ellinger J, Kahl P, von der Gathen J, Heukamp LC, Gutgemann I, Walter B, Hofstadter F, Bastian PJ, von Ruecker A, Muller SC and Rogenhofer S (2012) Global histone H3K27 methylation levels are different in localized and metastatic prostate cancer. *Cancer investigation* **30**:92-97.

Elliott B, Millena AC, Matyunina L, Zhang M, Zou J, Wang G, Zhang Q, Bowen N, Eaton V, Webb G, Thompson S, McDonald J and Khan S (2019) Essential role of JunD in cell proliferation is mediated via MYC signaling in prostate cancer cells. *Cancer letters* **448**:155-167.

Fan L, Peng G, Sahgal N, Fazli L, Gleave M, Zhang Y, Hussain A and Qi J (2016) Regulation of c-Myc expression by the histone demethylase JMJD1A is essential for prostate cancer cell growth and survival. *Oncogene* **35**:2441-2452.

Felsher DW and Bishop JM (1999) Reversible tumorigenesis by MYC in hematopoietic lineages.
Molecular cell **4**:199-207.

Fleming WH, Hamel A, MacDonald R, Ramsey E, Pettigrew NM, Johnston B, Dodd JG and Matusik
RJ (1986) Expression of the c-myc protooncogene in human prostatic carcinoma and benign
prostatic hyperplasia. *Cancer research* **46**:1535-1538.

García-Gutiérrez L, Delgado MD and León J (2019) MYC Oncogene Contributions to Release of Cell
Cycle Brakes. *Genes* **10**.

Giacinti C and Giordano A (2006) RB and cell cycle progression. *Oncogene* **25**:5220-5227.

Graça I, Pereira-Silva E, Henrique R, Packham G, Crabb SJ and Jerónimo C (2016) Epigenetic
modulators as therapeutic targets in prostate cancer. *Clinical epigenetics* **8**:98.

Hao S and Baltimore D (2009) The stability of mRNA influences the temporal order of the induction
of genes encoding inflammatory molecules. *Nature immunology* **10**:281-288.

Hashizume R, Andor N, Ihara Y, Lerner R, Gan H, Chen X, Fang D, Huang X, Tom MW, Ngo V,
Solomon D, Mueller S, Paris PL, Zhang Z, Petritsch C, Gupta N, Waldman TA and James CD
(2014) Pharmacologic inhibition of histone demethylation as a therapy for pediatric brainstem
glioma. *Nature medicine* **20**:1394-1396.

He W, Zhang MG, Wang XJ, Zhong S, Shao Y, Zhu Y and Shen ZJ (2013) KAT5 and KAT6B are in
positive regulation on cell proliferation of prostate cancer through PI3K-AKT signaling.
International journal of clinical and experimental pathology **6**:2864-2871.

Hess-Stumpp H (2005) Histone deacetylase inhibitors and cancer: from cell biology to the clinic.
European journal of cell biology **84**:109-121.

Hong S, Cho YW, Yu LR, Yu H, Veenstra TD and Ge K (2007) Identification of JmjC domain-
containing UTX and JMJD3 as histone H3 lysine 27 demethylases. *Proceedings of the
National Academy of Sciences of the United States of America* **104**:18439-18444.

Iwata T, Schultz D, Hicks J, Hubbard GK, Mutton LN, Lotan TL, Bethel C, Lotz MT,
Yegnasubramanian S, Nelson WG, Dang CV, Xu M, Anele U, Koh CM, Bieberich CJ and De
Marzo AM (2010) MYC overexpression induces prostatic intraepithelial neoplasia and loss of
Nkx3.1 in mouse luminal epithelial cells. *PloS one* **5**:e9427.

Jain M, Arvanitis C, Chu K, Dewey W, Leonhardt E, Trinh M, Sundberg CD, Bishop JM and Felsher DW (2002) Sustained loss of a neoplastic phenotype by brief inactivation of MYC. *Science (New York, NY)* **297**:102-104.

Jerónimo C, Bastian PJ, Bjartell A, Carbone GM, Catto JW, Clark SJ, Henrique R, Nelson WG and Shariat SF (2011) Epigenetics in prostate cancer: biologic and clinical relevance. *European urology* **60**:753-766.

Jung SH, Shin S, Kim MS, Baek IP, Lee JY, Lee SH, Kim TM, Lee SH and Chung YJ (2016) Genetic Progression of High Grade Prostatic Intraepithelial Neoplasia to Prostate Cancer. *European urology* **69**:823-830.

Karanikolas BD, Figueiredo ML and Wu L (2010) Comprehensive Evaluation of the Role of EZH2 in the Growth, Invasion, and Aggression of a Panel of Prostate Cancer Cell Lines. *The Prostate* **70**:675-688.

Ke XS, Qu Y, Rostad K, Li WC, Lin B, Halvorsen OJ, Haukaas SA, Jonassen I, Petersen K, Goldfinger N, Rotter V, Akslen LA, Oyan AM and Kalland KH (2009) Genome-wide profiling of histone h3 lysine 4 and lysine 27 trimethylation reveals an epigenetic signature in prostate carcinogenesis. *PloS one* **4**:e4687.

Kruidenier L, Chung C, Cheng Z, Liddle J, Che K, Joberty G, Bantscheff M, Bountra C, Bridges A, Diallo H, Eberhard D, Hutchinson S, Jones E, Katso R, Leveridge M, Mander PK, Mosley J, Ramirez-Molina C, Rowland P, Schofield CJ, Sheppard RJ, Smith JE, Swales C, Tanner R, Thomas P, Tumber A, Drewes G, Oppermann U, Patel DJ, Lee K and Wilson DM (2012) A selective jumonji H3K27 demethylase inhibitor modulates the proinflammatory macrophage response. *Nature* **488**:404-408.

Lin CY, Wang BJ, Chen BC, Tseng JC and Jiang SS (2019) Histone Demethylase KDM4C Stimulates the Proliferation of Prostate Cancer Cells via Activation of AKT and c-Myc. **11**.

Mandal C, Kim SH, Kang SC, Chai JC, Lee YS, Jung KH and Chai YG (2017) GSK-J4-Mediated Transcriptomic Alterations in Differentiating Embryoid Bodies. *Molecules and Cells* **40**:737-751.

Mateyak MK, Obaya AJ and Sedivy JM (1999) c-Myc regulates cyclin D-Cdk4 and -Cdk6 activity but affects cell cycle progression at multiple independent points. *Molecular and cellular biology* **19**:4672-4683.

Meškytė EM and Keskas S (2020) MYC as a Multifaceted Regulator of Tumor Microenvironment Leading to Metastasis. **21**.

Miremadi A, Oestergaard MZ, Pharoah PD and Caldas C (2007) Cancer genetics of epigenetic genes. *Human molecular genetics* **16 Spec No 1**:R28-49.

Morozov VM, Li Y, Clowers MM and Ishov AM (2017) Inhibitor of H3K27 demethylase JMJD3/UTX GSK-J4 is a potential therapeutic option for castration resistant prostate cancer. *Oncotarget* **8**:62131-62142.

Morten BC, Scott RJ and Avery-Kiejda KA (2016) Comparison of Three Different Methods for Determining Cell Proliferation in Breast Cancer Cell Lines. *Journal of visualized experiments : JoVE.*

Ngollo M, Dagdemir A, Judes G, Kemeny JL, Penault-Llorca F, Boiteux JP, Lebert A, Bignon YJ, Guy L and Bernard-Gallon D (2014) Epigenetics of prostate cancer: distribution of histone H3K27me3 biomarkers in peri-tumoral tissue. *Omics : a journal of integrative biology* **18**:207-209.

Ngollo M, Lebert A, Daures M, Judes G, Rifai K, Dubois L, Kemeny JL, Penault-Llorca F, Bignon YJ, Guy L and Bernard-Gallon D (2017) Global analysis of H3K27me3 as an epigenetic marker in prostate cancer progression. *BMC cancer* **17**:261.

Ntziachristos P, Tsirigos A, Welstead GG, Trimarchi T, Bakogianni S, Xu L, Loizou E, Holmfeldt L, Strikoudis A, King B, Mullenders J, Becksfort J, Nedjic J, Paietta E, Tallman MS, Rowe JM, Tonon G, Satoh T, Kruidenier L, Prinjha R, Akira S, Van Vlierberghe P, Ferrando AA, Jaenisch R, Mullighan CG and Aifantis I (2014) Contrasting roles of histone 3 lysine 27 demethylases in acute lymphoblastic leukaemia. *Nature* **514**:513-517.

Ohguchi H, Harada T and Sagawa M (2017) KDM6B modulates MAPK pathway mediating multiple myeloma cell growth and survival. **31**:2661-2669.

Pan H, Zhu Y, Wei W, Shao S and Rui X (2018) Transcription factor FoxM1 is the downstream target of c-Myc and contributes to the development of prostate cancer. *World journal of surgical oncology* **16**:59.

Pelengaris S, Littlewood T, Khan M, Elia G and Evan G (1999) Reversible activation of c-Myc in skin: induction of a complex neoplastic phenotype by a single oncogenic lesion. *Molecular cell* **3**:565-577.

Perez-Roger I, Kim SH, Griffiths B, Sewing A and Land H (1999) Cyclins D1 and D2 mediate myc-induced proliferation via sequestration of p27(Kip1) and p21(Cip1). *The EMBO journal* **18**:5310-5320.

Philipp A, Schneider A, Väsrik I, Finke K, Xiong Y, Beach D, Alitalo K and Eilers M (1994) Repression of cyclin D1: a novel function of MYC. *Molecular and cellular biology* **14**:4032-4043.

Rebello RJ, Pearson RB, Hannan RD and Furic L (2017) Therapeutic Approaches Targeting MYC-Driven Prostate Cancer. *Genes* **8**.

Seligson DB, Horvath S, Shi T, Yu H, Tze S, Grunstein M and Kurdistani SK (2005) Global histone modification patterns predict risk of prostate cancer recurrence. *Nature* **435**:1262-1266.

Sha J, Han Q, Chi C, Zhu Y, Pan J, Dong B, Huang Y, Xia W and Xue W (2020) Upregulated KDM4B promotes prostate cancer cell proliferation by activating autophagy. **235**:2129-2138.

Sharma A, Comstock CE, Knudsen ES, Cao KH, Hess-Wilson JK, Morey LM, Barrera J and Knudsen KE (2007) Retinoblastoma tumor suppressor status is a critical determinant of therapeutic response in prostate cancer cells. *Cancer research* **67**:6192-6203.

Shin YJ and Kim JH (2012) The role of EZH2 in the regulation of the activity of matrix metalloproteinases in prostate cancer cells. *PloS one* **7**:e30393.

Shukeir N, Pakneshan P, Chen G, Szyf M and Rabbani SA (2006) Alteration of the methylation status of tumor-promoting genes decreases prostate cancer cell invasiveness and tumorigenesis in vitro and in vivo. *Cancer research* **66**:9202-9210.

Smith PK, Krohn RI, Hermanson GT, Mallia AK, Gartner FH, Provenzano MD, Fujimoto EK, Goeke NM, Olson BJ and Klenk DC (1985) Measurement of protein using bicinchoninic acid. *Analytical biochemistry* **150**:76-85.

Solomon DL, Philipp A, Land H and Eilers M (1995) Expression of cyclin D1 mRNA is not upregulated by Myc in rat fibroblasts. *Oncogene* **11**:1893-1897.

Sui A, Xu Y, Li Y, Hu Q, Wang Z, Zhang H, Yang J, Guo X and Zhao W (2017) The pharmacological role of histone demethylase JMJD3 inhibitor GSK-J4 on glioma cells. *Oncotarget* **8**:68591-68598.

Terashima M, Ishimura A, Yoshida M, Suzuki Y, Sugano S and Suzuki T (2010) The tumor suppressor Rb and its related Rbl2 genes are regulated by Utx histone demethylase. *Biochemical and biophysical research communications* **399**:238-244.

Tomlins SA, Mehra R, Rhodes DR, Cao X, Wang L, Dhanasekaran SM, Kalyana-Sundaram S, Wei JT, Rubin MA, Pienta KJ, Shah RB and Chinnaiyan AM (2007) Integrative molecular concept modeling of prostate cancer progression. *Nature genetics* **39**:41-51.

Topacio BR, Zatulovskiy E, Cristea S, Xie S, Tambo CS, Rubin SM, Sage J, Kõivomägi M and Skotheim JM (2019) Cyclin D-Cdk4,6 Drives Cell-Cycle Progression via the Retinoblastoma Protein's C-Terminal Helix. *Molecular cell* **74**:758-770.e754.

Turner BM (1993) Decoding the nucleosome. *Cell* **75**:5-8.

Varambally S, Dhanasekaran SM, Zhou M, Barrette TR, Kumar-Sinha C, Sanda MG, Ghosh D, Pienta KJ, Sewalt RG, Otte AP, Rubin MA and Chinnaiyan AM (2002) The polycomb group protein EZH2 is involved in progression of prostate cancer. *Nature* **419**:624-629.

Venkateswaran N (2020) MYC leads the way. *International journal of molecular sciences* **11**:86-94.

Vieira FQ, Costa-Pinheiro P, Ramalho-Carvalho J, Pereira A, Menezes FD, Antunes L, Carneiro I, Oliveira J, Henrique R and Jeronimo C (2014) Deregulated expression of selected histone methylases and demethylases in prostate carcinoma. *Endocrine-related cancer* **21**:51-61.

Wu Y, Sarkissyan M and Vadgama JV (2015) Epigenetics in breast and prostate cancer. *Methods in molecular biology (Clifton, NJ)* **1238**:425-466.

Xiang Y, Zhu Z, Han G, Lin H, Xu L and Chen CD (2007) JMJD3 is a histone H3K27 demethylase. *Cell research* **17**:850-857.

Yildirim-Buharalioglu G, Bond M, Sala-Newby GB, Hindmarch CC and Newby AC (2017) Regulation of Epigenetic Modifiers, Including KDM6B, by Interferon-gamma and Interleukin-4 in Human Macrophages. *Frontiers in immunology* **8**:92.

Yu Q, Ciemerych MA and Sicinski P (2005) Ras and Myc can drive oncogenic cell proliferation through individual D-cyclins. *Oncogene* **24**:7114-7119.

Zhang M, Wang Q, Sun X, Yin Q, Chen J, Xu L and Xu C (2020) β(2) -adrenergic receptor signaling drives prostate cancer progression by targeting the Sonic hedgehog-Gli1 signaling activation. **80**:1328-1340.

Zhao L, Zhang Y, Gao Y, Geng P, Lu Y, Liu X, Yao R, Hou P, Liu D, Lu J and Huang B (2015) JMJD3 promotes SAHF formation in senescent WI38 cells by triggering an interplay between demethylation and phosphorylation of RB protein. *Cell death and differentiation* **22**:1630-1640.

FOOTNOTES

The author declares that there is no conflict of interest.

FIGURE LEGENDS

Figure 1: **Changes in constitutive KDM6A and KDM6B levels in PCa metastatic cell lines.**

Changes in steady state mRNA levels of KDM6A and KDM6B, protein level of KDM6A in human

PCa metastatic cell lines LNCaP, PC3 and DU145 compared to BPH-1. Total RNA and protein were

extracted from 48 h incubated BPH-1, LNCaP, PC3 and DU145 cells and subjected to RT-qPCR for

(A) KDM6A, (B) KDM6B, (C) 36B4 mRNA levels and Western blotting for (D) KDM6A protein

33

level, respectively. For A, B and C results are expressed as mRNA relative to BPH-1 (control cell line). For D, the densitometry results are normalized against GAPDH. Data are presented as the mean ± S.D. from three independent experiments (n=3). P values were calculated using a one-way ANOVA with Dunnett's multiple comparisons tests. ** indicates p<0.01, *** indicates p<0.001.

Figure 2: Effect of KDM6 inhibitor, GSK-J4 dose response. Change in protein levels of global H3K27me$_3$ and steady state mRNA levels of CCND1, SLC4A4, MYB and 36B4 by GSK-J4. LNCaP cells were treated with 4, 10 or 30 μM GSK-J4 or vehicle (DMSO) for 18 h in FBS free or 1 % FBS supplemented medium. (A) Global levels of H3K27me$_3$ were measured by Western blotting (n=1) and levels of mRNA relative to DMSO were determined by RT-qPCR for (B) CCND1, (C) SLC4A4, (D) MYB, (E) 36B4. Data are presented as the mean ± S.D. from three independent experiments (n=3). P values were calculated using a one-way ANOVA with Dunnett's multiple comparisons tests. [#] indicates p<0.05, [###] indicates p<0.001 vs FBS free DMSO. * indicates p<0.05, ** indicates p<0.01, *** indicates p<0.001 vs 1 % FBS DMSO.

Figure 3: Effect of KDM6 inhibitor, GSK-J4 time course. Change in protein levels of global H3K27me$_3$ and steady state mRNA levels of CCND1, SLC4A4, MYB and 36B4. LNCaP cells were treated with 30 μM GSK-J4 or vehicle (DMSO) for 6, 18, 24 or 48 h in 1 % FBS supplemented medium. (A) Global levels of H3K27me$_3$ were measured by Western blotting (n=1) and levels of mRNA relative to DMSO were determined by RT-qPCR for (B) CCND1, (C) SLC4A4, (D) MYB, (E) 36B4. Data are presented as the mean ± S.D. from three independent experiments (n=3). P values were calculated using a two-way ANOVA with Bonferroni's multiple comparisons tests. *** indicates p<0.001.

Figure 4: Validation of c-MYC levels by GSK-J4. LNCaP cells were treated with 30 μM GSK-J4 or vehicle (DMSO) for 18 h in 1 % FBS supplemented medium. (A) RT^2 profiler PCR array for Human Tumor Metastasis genes in LNCaP cells after GSK-J4. The scatter plot of the GSK-J4 vs DMSO samples indicates the validity of the experiment. (B) Levels of c-MYC steady state mRNA and pre-spliced c-MYC mRNAs relative to DMSO were determined by RT-qPCR. (C) Levels of c-MYC

protein were measured by Western blotting. The densitometry results are normalized against GAPDH. Data are presented as the mean ± S.D. from three independent experiments (n=3). *P* values were calculated using two tail unpaired t test. * indicates p<0.05, ** indicates p<0.01, *** indicates p<0.001.

Figure 5: Effect of siRNA mediated silencing of KDM6A and KDM6B. LNCaP cells were plated at density of $6x10^4$ cells for each well of 24 well plates and incubated for 24 h followed by transfection with 20 pmol of each individual siRNA for 72 h. The levels of mRNAs for (A) KDM6A and KDM6B, (C) c-MYC and (D) 36B4 were measured in cells transfected with siKDM6A, siKDM6B, individually or together were normalized against those with si Negative Control (siNegC) as control. The levels of protein for (B) KDM6A (n=3) and (E) c-MYC (n=1) were measured in cells transfected with siKDM6A, siKDM6B, individually or together. The densitometry results are normalized against GAPDH. Data are presented as the mean ± S.D. from three independent experiments (n=3). *P* values were calculated using a one-way ANOVA with Dunnett's multiple comparisons tests. * indicates p<0.05, ** indicates p<0.01, *** indicates p<0.001.

Figure 6: Effect of KDM6A/B silencing pharmacologically or with siRNA on CCND1 and pRb levels (A-D). Effect of GSK-J4 on proliferation of LNCaP cells (E-F). LNCaP cells were treated with 30 µM GSK-J4 or vehicle (DMSO) for 18 h in 1 % FBS supplemented medium. Protein levels of (A) CCND1 and (C) pRb were measured by Western blotting. LNCaP cells were transfected with 20 pmol of each individual siRNA for 72h. The levels of mRNA for (B) CCND1 and levels of protein for (D) pRb were measured in cells transfected with siKDM6A, siKDM6B, individually or together. mRNA results were normalized against those with si Negative Control (siNegC) as control. The densitometry results are normalized against GAPDH. 30 µM GSK-J4 or DMSO (vehicle) treated LNCaP cells were either added CellTiter 96® AQ$_{ueous}$ One Solution Reagent and incubated for further 3 h or counted utilizing Trypan blue exclusion and results were represented as percentage of relative proliferation (E), total cell number (F), and trypan blue positive cell number to DMSO (G), respectively. Data are presented as the mean ± S.D. from three independent experiments (n=3). *P* values were calculated using either two tail unpaired t test or one-way ANOVA with Dunnett's

multiple comparisons tests as appropriate. * indicates $p<0.05$, ** indicates $p<0.01$, *** indicates $p<0.001$.

Table 1: **Primers used for RT-qPCR**

Gene name	Sequences for RT-PCR from 5' to 3'	
CCND1	forward	CCAGAGGCGGAGGAGAACAAACAG
	reverse	CCATGGAGGGCGGATTGGAAATGA

c-MYC	forward	CCTCTGTTGAAATGGGTCTGGGGG
	reverse	CACCTGCCTTCTGCCATTCCTTCT
KDM6A	forward	CCATGAACACAGCACAGCAGGCAT
	reverse	CTTGGCAGGACTGGACAGGTCATC
KDM6B	forward	GCAACCACCGCCTGCGTGCCTTAC
	reverse	CGGGAATGCCTGGGTTCGGCTCCA
MYB	forward	ACAGAACCACACATGCAGCTACCC
	reverse	ATGGAGTGGAGTGGTGTTCTCCCA
SLC4A4	forward	AGGATGGAGGATGAAGCTGTCCTG
	reverse	TCCGATGTAAATGGTATGGTGGCCT
pre-spliced c-MYC	forward	CCGCACCAAGACCCCTTTAACTCA
	reverse	AAATACGGCTGCACCGAGTCGTAG
36B4	forward	GCCAGCGAAGCCACGCTGCTGAAC
	reverse	CGAACACCTGCTGGATGACCAGCCC

Table 2: **Changes in expression of human tumor metastasis genes by GSK-J4.** LNCaP cells were treated with 30 μM GSK-J4 or DMSO (vehicle) for 18 h in 1 % FBS supplemented medium. Extracted RNA samples were subjected to analysis by the Human Tumor Metastasis RT² Profiler PCR Array

(QIAGEN). *P* values were calculated alone without any correction based on normalisation against

RPLP0 with 2 fold change as a cut off value and using a Student's t-test of the replicate $2^{(-\Delta C_T)}$ values for

each gene in the control group (DMSO) and treatment group (GSK-J4) (* indicates $p<0.05$, ** indicates

$p< 0.01$, *** indicates $p< 0.001$, n=3 independent experiment). The p-value calculation used is based on

parametric, unpaired, two-sample equal variance, two-tailed distribution. Because GSK-J4 is a selective

inhibitor of KDM6 family demethylases, GSK-J4 down-regulated genes (c-MYC, NF2, CTBP1,

EPHB2, PLAUR), which are possible targets for KDM6A and KDM6B, were shown in bold in Table 2.

Nomenclature: c-MYC, V-myc myelocytomatosis viral oncogene homolog (avian); NF2,

Neurofibromin 2 (merlin); CTBP1, C-terminal binding protein 1; EPHB2, EPH receptor B2; PLAUR,

Plasminogen activator, urokinase receptor; MMP13, Matrix metallopeptidase 13 (collagenase 3),

MMP10, Matrix metallopeptidase 10 (stromelysin 2); VEGFA, Vascular endothelial growth factor A;

RORB, RAR-related orphan receptor B.

GENE	FOLD CHANGE	p VALUE	Lower-Upper 95 % CI	FUNCTION
c-MYC	**0.27****	0.0011	0.24-0.30	Cell Cycle Arrest & Checkpoints Cell Growth & Proliferation Transcription Factors & Regulators
NF2	**0.35***	0.0160	0.02-0.68	Regulation of the Cell Cycle Regulation of Cell Proliferation
CTBP1	**0.41***	0.0289	0.12-0.70	Regulation of Cell Proliferation
EPHB2	**0.44***	0.0243	0.28-0.60	Cell Surface Receptors Cell Growth & Proliferation
PLAUR	**0.48***	0.0122	0.45-0.51	Cell Surface Receptors Cell Growth & Proliferation
MMP13	3.51*	0.0142	3.45-3.57	Extracellular Matrix Proteases
MMP10	4.89*	0.0119	1.5-8.4	Extracellular Matrix Proteases
VEGFA	8.69***	0.0004	5.3-12.1	Cell Adhesion Molecules Regulation of the Cell Cycle Cell Growth & Proliferation

RORB	19.88**	0.0026	7.8-32.7	Cell Surface Receptors
				Cell Growth & Proliferation
				Transcription Factors & Regulators
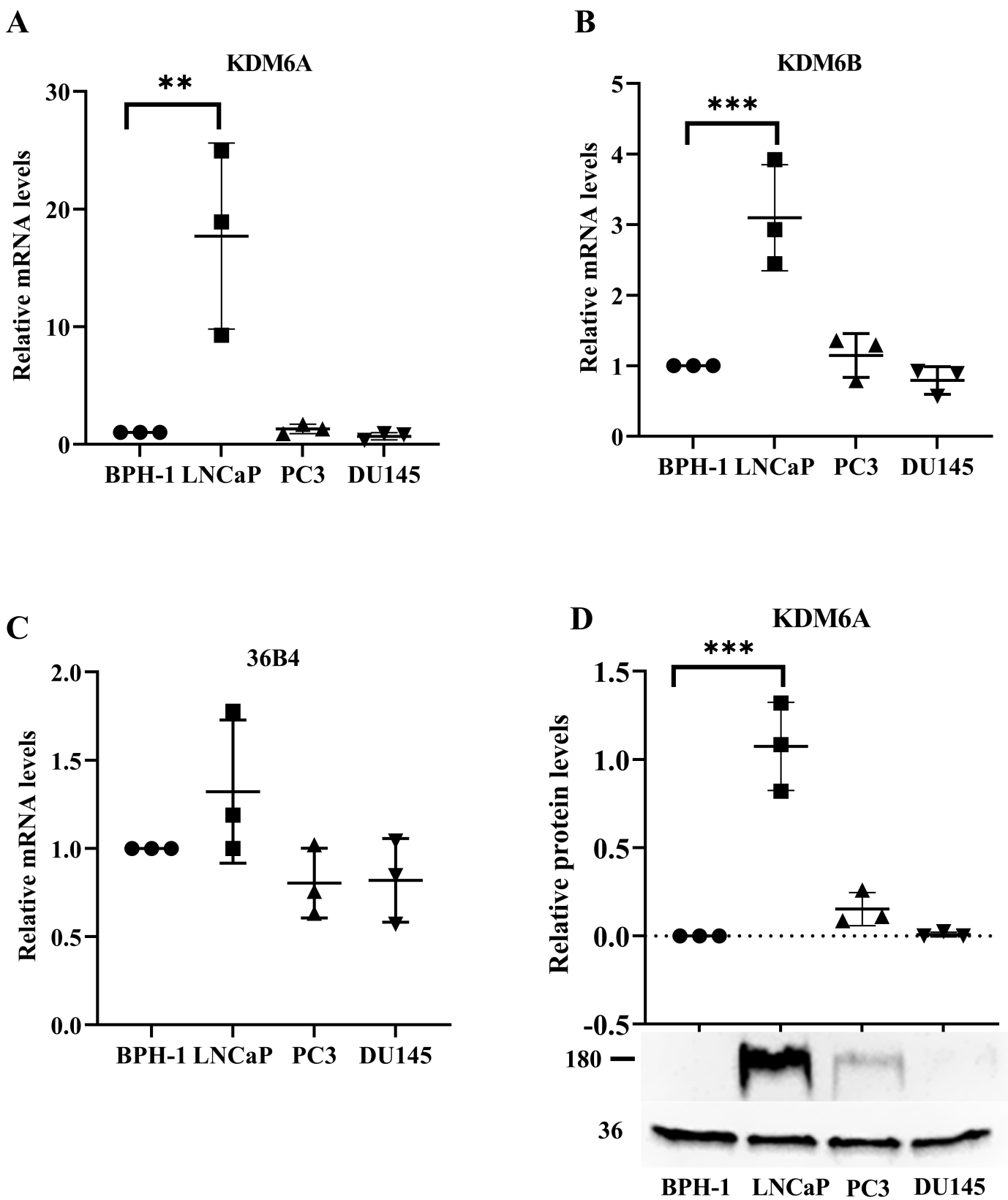
FIGURE 1

FIGURE 2

FIGURE 3

A

GSK-J4 vs DMSO

→ c-MYC

B

c-MYC

● mRNA ▲ pre-spliced mRNA

*** **

C

c-MYC

*

63 ―   c-MYC

36   GAPDH

DMSO   GSK-J4
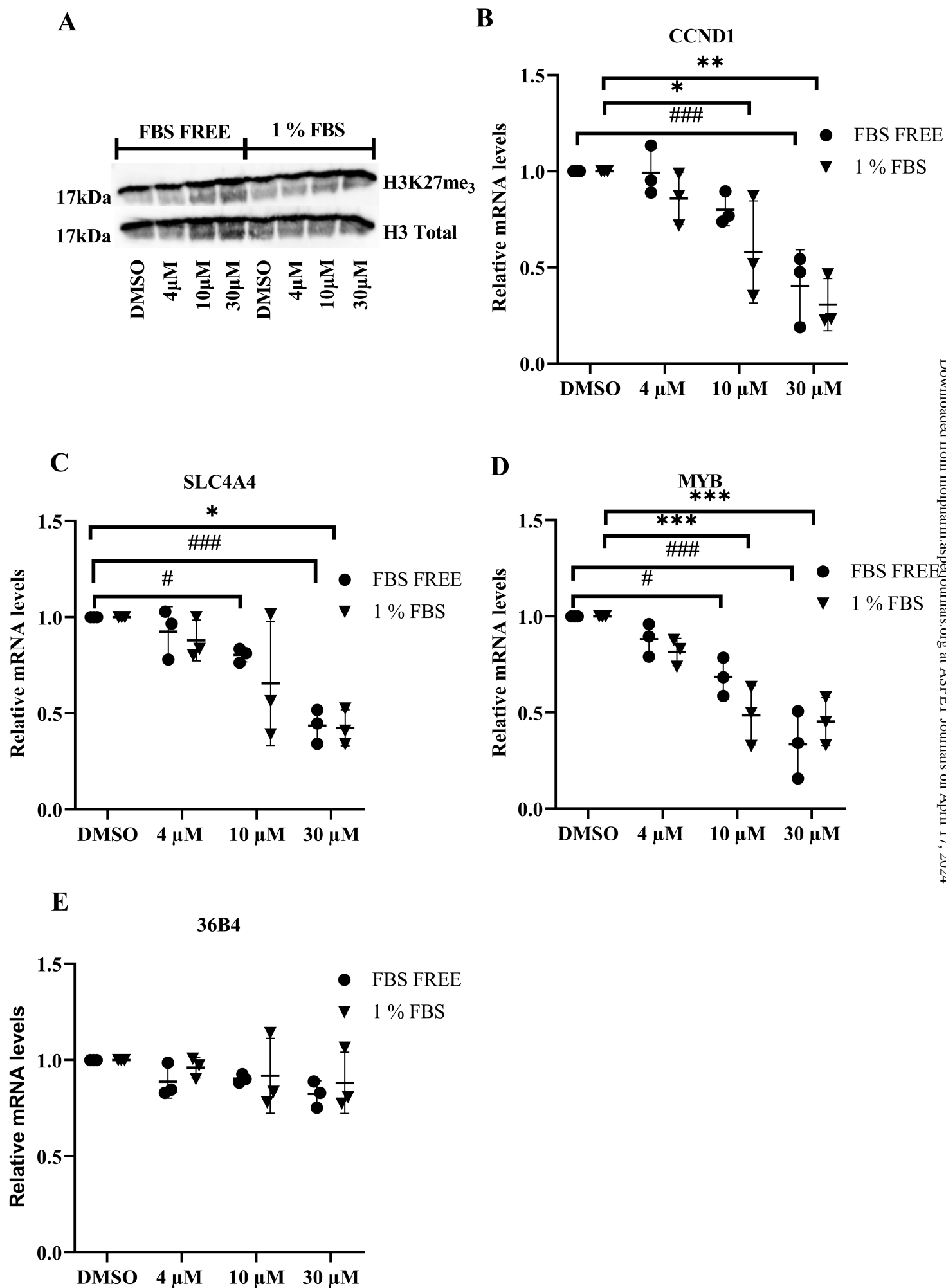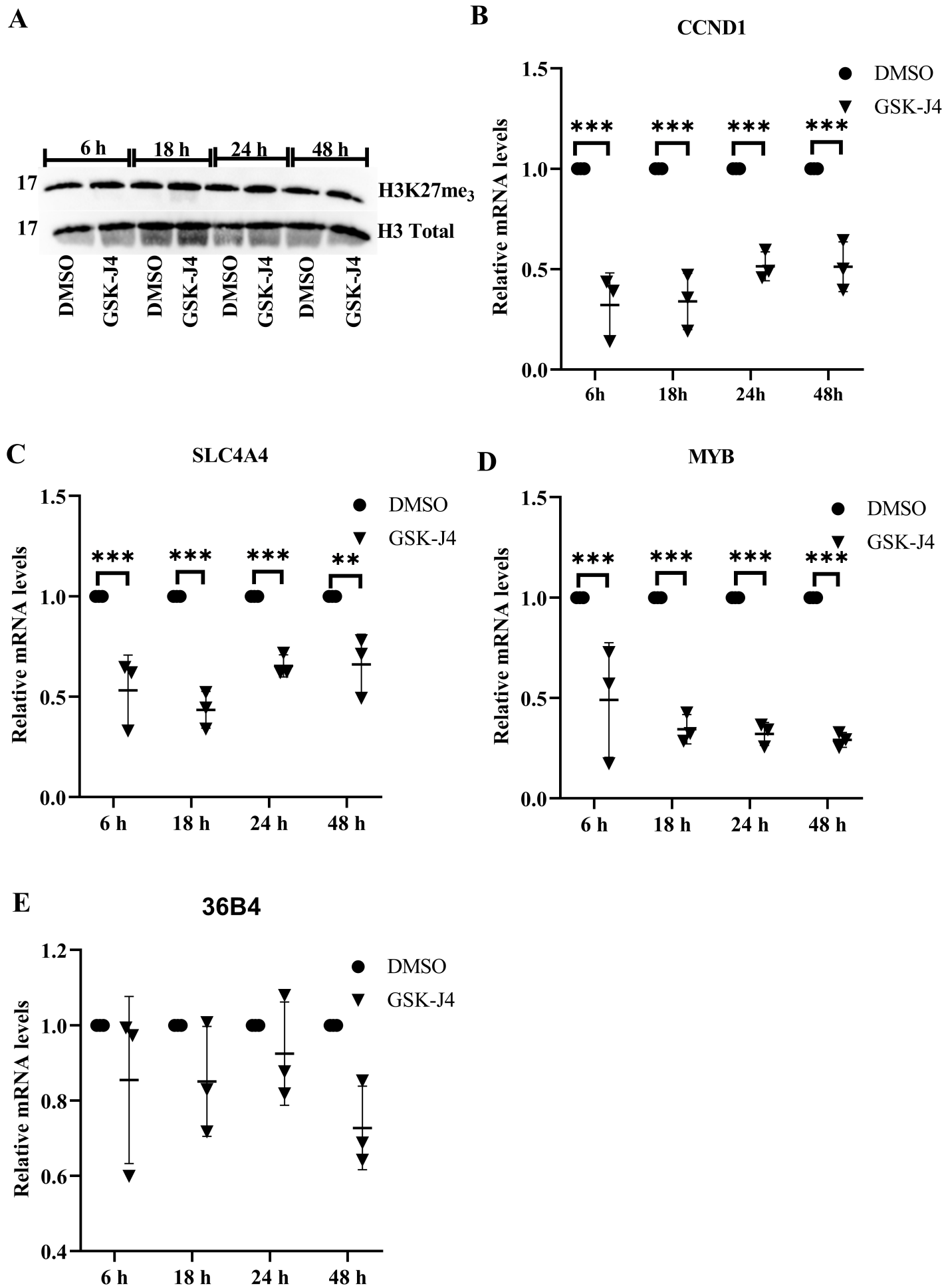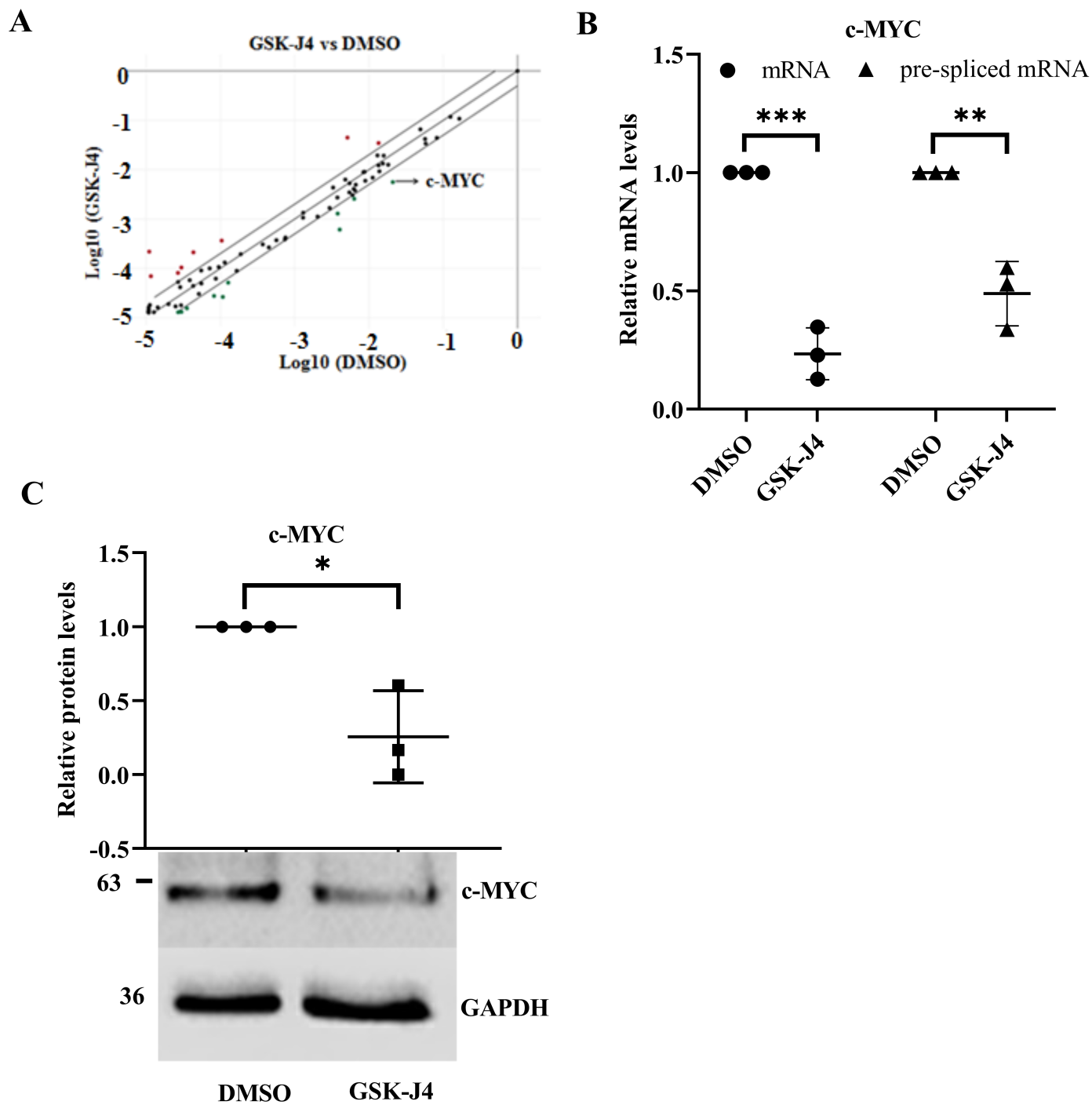
FIGURE 4

FIGURE 5

FIGURE 6